Comparison between DAMA/LIBRA and COSINE-100 in the light of Quenching Factors

The COSINE-100 Collaboration
Y. J. Ko[a] G. Adhikari[b] P. Adhikari[b,1] E. Barbosa de Souza[c]
N. Carlin[d] J. J. Choi[e] S. Choi[e] M. Djamal[f] A. C. Ezeribe[g]
C. Ha[a] I. S. Hahn[h] E. J. Jeon[a] J. H. Jo[c] W. G. Kang[a]
M. Kauer[j] G. S. Kim[k] H. Kim[a] H. J. Kim[k] K. W. Kim[a]
N. Y. Kim[a] S. K. Kim[e] Y. D. Kim[a,b,m] Y. H. Kim[a,l,m] E. K. Lee[a]
H. S. Lee[a,m] J. Lee[a] J. Y. Lee[k] M. H. Lee[a,m] S. H. Lee[m,a]
D. S. Leonard[a] W. A. Lynch[g] B. B. Manzato[d] R. H. Maruyama[c]
R. J. Neal[g] S. L. Olsen[a] B. J. Park[m,a] H. K. Park[n] H. S. Park[l]
K. S. Park[a] R. L. C. Pitta[d] H. Prihtiadi[f] S. J. Ra[a] C. Rott[i]
K. A. Shin[a] A. Scarff[g] N. J. C. Spooner[g] W. G. Thompson[c]
L. Yang[o] and G. H. Yu[i]

[a]Center for Underground Physics, Institute for Basic Science (IBS), Daejeon 34126, Republic of Korea

[b]Department of Physics, Sejong University, Seoul 05006, Republic of Korea

[c]Department of Physics and Wright Laboratory, Yale University, New Haven, CT 06520, USA

[d]Physics Institute, University of São Paulo, 05508-090, São Paulo, Brazil

[e]Department of Physics and Astronomy, Seoul National University, Seoul 08826, Republic of Korea

[f]Department of Physics, Bandung Institute of Technology, Bandung 40132, Indonesia

[g]Department of Physics and Astronomy, University of Sheffield, Sheffield S3 7RH, United Kingdom

[h]Department of Science Education, Ewha Womans University, Seoul 03760, Republic of Korea

[i]Department of Physics, Sungkyunkwan University, Suwon 16419, Republic of Korea

[j]Department of Physics and Wisconsin IceCube Particle Astrophysics Center, University of Wisconsin-Madison, Madison, WI 53706, USA

[k]Department of Physics, Kyungpook National University, Daegu 41566, Republic of Korea

[l]Korea Research Institute of Standards and Science, Daejeon 34113, Republic of Korea

[1]Present address : Department of Physics, Carleton University, Ottawa, ON K1S 5B6, Canada

[m]IBS School, University of Science and Technology (UST), Daejeon 34113, Republic of Korea

[n]Department of Accelerator Science, Korea University, Sejong 30019, Republic of Korea

[o]Department of Physics, University of Illinois at Urbana-Champaign, Urbana, IL 61801, USA

E-mail: yjko@ibs.re.kr, kwkim@ibs.re.kr, hyunsulee@ibs.re.kr

Abstract. There is a long standing debate about whether or not the annual modulation signal reported by the DAMA/LIBRA collaboration is induced by Weakly Interacting Massive Particles (WIMP) in the galaxy's dark matter halo scattering from nuclides in their NaI(Tl) crystal target/detector. This is because regions of WIMP-mass vs. WIMP-nucleon cross-section parameter space that can accommodate the DAMA/LIBRA-phase1 modulation signal in the context of the standard WIMP dark matter galactic halo and isospin-conserving (canonical), spin-independent (SI) WIMP-nucleon interactions have been excluded by many of other dark matter search experiments including COSINE-100, which uses the same NaI(Tl) target/detector material. Moreover, the recently released DAMA/LIBRA-phase2 results are inconsistent with an interpretation as WIMP-nuclide scattering via the canonical SI interaction and prefer, instead, isospin-violating or spin-dependent interactions. Dark matter interpretations of the DAMA/LIBRA signal are sensitive to the NaI(Tl) scintillation efficiency for nuclear recoils, which is characterized by so-called quenching factors (QF), and the QF values used in previous studies differ significantly from recently reported measurements, which may have led to incorrect interpretations of the DAMA/LIBRA signal. In this article, the compatibility of the DAMA/LIBRA and COSINE-100 results, in light of the new QF measurements is examined for different possible types of WIMP-nucleon interactions. The resulting allowed parameter space regions associated with the DAMA/LIBRA signal are explicitly compared with 90% confidence level upper limits from the initial 59.5 day COSINE-100 exposure. With the newly measured QF values, the allowed 3σ regions from the DAMA/LIBRA data are still generally excluded by the COSINE-100 data.

Contents

1 Introduction

A number of astrophysical observations provide evidence that the dominant matter component of the universe is not ordinary matter, but rather non-baryonic dark matter [1, 2]. Weakly Interacting Massive Particles (WIMPs) are particle dark matter candidates [3–5] that have been the subject of extensive searches by direct detection, indirect detection, and collider experiments, with no success [6].

The one exception is the long-standing observation by the DAMA/LIBRA collaboration of an annual modulation in the low-energy event rate in an underground array of low-background NaI(Tl) detectors. Although this signal has persisted throughout more than 20 years of investigation [7–11], its interpretation as being due to WIMP-nucleus scattering in the specific context of the standard galactic WIMP halo model [12, 13], has been the subject of a continuing debate. This is because the WIMP-nucleon cross sections inferred from the DAMA/LIBRA modulation are in conflict with limits from other experiments that directly measure the total, time integrated rate of nuclear recoils [14–24]. An unambiguous verification of the DAMA/LIBRA signal by independent experiments using the same NaI(Tl) crystal target material is mandatory. Experimental efforts by several groups using the same NaI(Tl) target medium are currently underway [25–30].

COSINE-100, located at the Yangyang underground laboratory in South Korea, is one of the experiments aimed at testing the DAMA/LIBRA results with a NaI(Tl) crystal detector/target [27]. The experiment, which began data taking in 2016, utilizes eight low-background NaI(Tl) scintillating crystals [31] arranged in a 4×2 array, with a total target mass of 106 kg. Each crystal is coupled to two photomultiplier tubes (PMTs) to measure the amount of deposited energy in the crystal. The crystal assemblies are immersed in 2,200 L of liquid scintillator, which allows for the identification and subsequent reduction of radioactive backgrounds observed in the crystals [32]. The liquid scintillator is surrounded by copper, lead, and plastic scintillators to reduce the background contribution from external radiation as well as tag cosmic-ray muons that transit the apparatus [33].

With the initial 59.5 live days exposure of COSINE-100, we reported our first WIMP dark matter search result [34] that excluded the 3σ region of allowed WIMP masses and cross sections that were associated with the DAMA/LIBRA-phase1 signal assuming canonical (isospin-conserving) spin-independent (SI) WIMP interactions in the specific context of the

standard WIMP galactic halo model [35]. Even though DAMA/LIBRA and COSINE-100 use the same NaI(Tl) target, there are differences. The DAMA/LIBRA signal is an annual modulation effect while the COSINE-100 result is based on the time averaged spectral shape [36]. Although the first modulation measurements from ANAIS-112 [37] and COSINE-100 [38] were recently released, both experiments still need a few more years of exposure to reach a modulation sensitivity that is sufficient to probe the DAMA/LIBRA signal directly [27, 29].

It is interesting to compare the DAMA/LIBRA annual modulation signal with the time-averaged rate considering specific models for the WIMP-nucleon interaction. This is especially the case for the time-averaged NaI(Tl) results from COSINE-100 [34]. While the DAMA/LIBRA-phase1 results used a 2 keVee (electron equivalent energy) energy threshold, the recent phase2 result has a lower threshold of 1 keVee [11]. The new low-threshold energy signal has a significantly worse goodness-of-fit for the canonical SI scattering scenario [39–41], suggesting that an isospin-violating model in which the WIMP-proton coupling is different from the WIMP-neutron coupling, or a spin-dependent (SD) interaction model are better suited for WIMP dark matter interpretations of the signal.

To make reliable comparison between the time-averaged rate and the annual modulation amplitude, a local distribution of dark matter particles is necessary. In this paper, we use standard galactic WIMP halo model [12, 13] that has the speed distribution associated with the Maxwell Botzmann,

$$f(\mathbf{v}, t) = \frac{1}{N_{\mathrm{esc}}} \ e^{-(v+v_{\mathrm{E}})^2/2\sigma_v^2}, \tag{1.1}$$

where N_{esc} is a normalization constant, v_E is the Earth velocity relative to the WIMP dark matter, and σ_v is the velocity dispersion. The standard halo parameterization is used with local dark matter density $\rho_\chi = 0.3 \ \mathrm{GeV/cm}^3$, $v_E = 232$ km/s, $\sqrt{2}\sigma_v = 220$ km/s and galactic escape velocity $v_{\mathrm{esc}} = 544$ km/s.

Astrophysical parameters related with dark matter local distribution have large uncertainties [42–44]. The adoption of various possibilities for the dark matter halo structures typically extends allowed parameter regions, as studied by DAMA/LIBRA [45]. If we consider various halo models that allow different modulation fraction to total rate, DAMA/LIBRA allowed regions will not be fully covered by the COSINE-100 data as examples shown in Refs. [36, 46]. This can be improved with larger dataset from COSINE-100 and ANAIS-112 in the future and analysis of data for the model independent annual modulations [27, 29]. However, it is still interesting to test the situation based on the widely used standard galactic halo model.

One noticeable issue with the interpretation of the DAMA/LIBRA obervation in terms of WIMP-nucleon interactions is the value of the nuclear-recoil quenching factor (QF). Quenching factors are the scintillation light yields for sodium and iodine recoils relative to those for γ/electron-induced radiation of the same energy. Most previous studies have used QF values reported by the DAMA/NaI collaboration in 1996 [47] (subsequently referred to as DAMA QF values), that were obtained by measuring the response of NaI(Tl) crystals to nuclear recoils induced by neutrons from a ^{252}Cf source. The measured responses are compared with the simulated neutron energy spectrum to obtain QF values with the assumption that they are independent of the energy of the recoiling nuclide: for sodium recoil energies between 6.4 and 97 keVnr (nuclear recoil energy), QF_{Na}=0.30±0.01; for iodine recoil energies between 22 and 330 keVnr, QF_{I}=0.09±0.01 [47]. Recently, results from more refined methods for measuring NaI(Tl) QF values that use monochromatic neutron beams have been reported [48–51]. In

these measurements, the detection of an elastically scattered neutron at a fixed angle relative to the incoming neutron beam direction provides an unambiguous knowledge of the energy transferred to the target nuclide. The QF values from these recent determinations differ significantly from the 1996 DAMA QF results, as shown in Fig. 1.

In this article, allowed regions in WIMP-nucleon cross-section and WIMP mass parameter space corresponding to the DAMA/LIBRA signal are presented for some of the different possible dark matter interactions that are discussed in Ref. [39] using the recently measured QF_{Na} and QF_I values. The DAMA/LIBRA-phase1 [10] and phase2 [11] data are used simultaneously for cases where a good quality-of-fit was obtained. The allowed regions from the DAMA/LIBRA data are explicitly compared with the 90% confidence level (CL) limits estimated from the 59.5 day COSINE-100 exposure [34]. For comparison, the same data are interpreted using the DAMA QF values. For all of the WIMP-nucleon interactions considered here, we find that the COSINE-100 data excludes the 3σ allowed regions associated with the DAMA/LIBRA data in the context of the standard WIMP galactic halo model.

2 Quenching factor model and implications for the interpretation of the DAMA/LIBRA signal

The electron-equivalent visible energy E_{ee} produced by recoil nuclei in scintillation detector is typically smaller than its true nuclear recoil energy E_R. The ratio of E_{ee} to E_R, the nuclear recoil quenching factor (QF), has to be externally evaluated in order to interpret results from dark matter search experiments that use scintillating crystal target/detectors. The DAMA/LIBRA collaboration measured QF values for sodium, QF_{Na}=0.3±0.01 averaged over 6.4 to 97 keVnr, and iodine, QF_I=0.09±0.01 averaged over 22 to 330 keVnr [47]. Several measurements in literature between 1994 and 2008, using mono-energetic neutrons produced by neutron generators, obtained consistent results as well [52–56].

However, recent measurements by Collar [48], Stiegler *etal*. [50], Xu *et al*. [49] and Joo *et al*. [51] reported significantly different results of strong E_R dependence as presented in Fig.1. Main difference of QF_{Na} behavior has arised at energy below 20 keVnr corresponding to approximately 2 keVee. Efficient noise rejection as well as correct evaluation of trigger and selection efficiencies are essential for proper estimation of the quenching factors in this domain [48, 49, 53]. Considering high light yield crystals and much precise determination of QF_{Na} in the new measurements [49–51], we only consider recent four QF_{Na} measurements for our modeling.

In order to parameterize the energy-dependent QF measurements, we use the formula from Lindhard *et al*. [57]:

$$f(E_R) = \frac{kg(\epsilon)}{1 + kg(\epsilon)}, \tag{2.1}$$

where $\epsilon = 11.5Z^{-7/3} E_R$, $k = 0.133Z^{2/3}A^{1/2}$, Z is the number of protons, and A is the number of nucleons. The function $g(\epsilon)$ is given by [12] to be:

$$g(\epsilon) = 3\epsilon^{0.15} + 0.7\epsilon^{0.6} + \epsilon. \tag{2.2}$$

The direct application of the Lindhard model to the NaI(Tl) crystals provides a poor match to the recently measured QF values. We, therefore, consider $k = p_0$ and $\epsilon = p_1 E_R$, where p_0 and p_1 are fit parameters. This modified Lindhard model well describes the recent measurements of QF_{Na} and QF_I as shown in Fig. 1 and the fit results are shown in Table 1. For

the QF_{Na} measurements, we do not directly use Collar's measurement due to its large uncertainties, which are covered by the other measurements. There are two QF_I measurements by Collar and Joo *et al.* as shown in Fig. 1 (b). In order to estimate the QF_I model, we use only the results from Joo *et al.*, because the measurement by Joo *et al.* covers that by Collar in terms of energy coverages as well as uncertainties.

Even though the new measurements have consistent energy dependence and lower QF values than those measured by DAMA, there are some mutual differences. These may be due to different environmental conditions such as temperature [58], analysis methods (including different charge integration windows), and different thallium doping concentration of the crystals used for the measurements. In applying these new QF values to the DAMA/LIBRA data, we consider these variations as a source of systematic uncertainty. The Joo *et al.* [51] results are taken as the central value with allowed systematical variations that span the range between the Xu *et al.* [49] and Stiegler *et al.* [50] measurements. Figure 1 (a) shows the three new QF measurement sets, each with its own fit based on the modified Lindhard model. Because of the fast increase of QF_{Na} in the Stiegler *et al.* measurements at energies higher than 19.6 keVnr, the lower bound of systematic uncertainties, denoted by a blue solid line in Fig. 1 (a), was taken to be the difference between the Xu *et al.* and Joo *et al.* measurements. In the case of the COSINE-100 data, the Joo *et al.* results were used because these measurements used a crystal from the same ingot, the same data aquisition system [59], and the same analysis framework as the COSINE-100 experimental data.

We use the modulation amplitude results from DAMA/LIBRA-phase1 [10] and phase2 [11], as rebinned in Ref. [39] and shown in Fig. 2. We built a χ^2 fitter to test the DAMA/LIBRA data against the modulation amplitude that is expected for the WIMP interaction under consideration. The energy resolution of the DAMA/LIBRA detector was taken from Refs. [60, 61]; the reported DAMA/LIBRA data is efficiency corrected. In order to obtain allowed regions in the WIMP mass vs. WIMP-proton cross-section parameter space, we implement a maximum likelihood method based on the likelihood ratio to fit for mass and cross section values. Confidence regions in these parameters are determined by examining variations of the likelihood
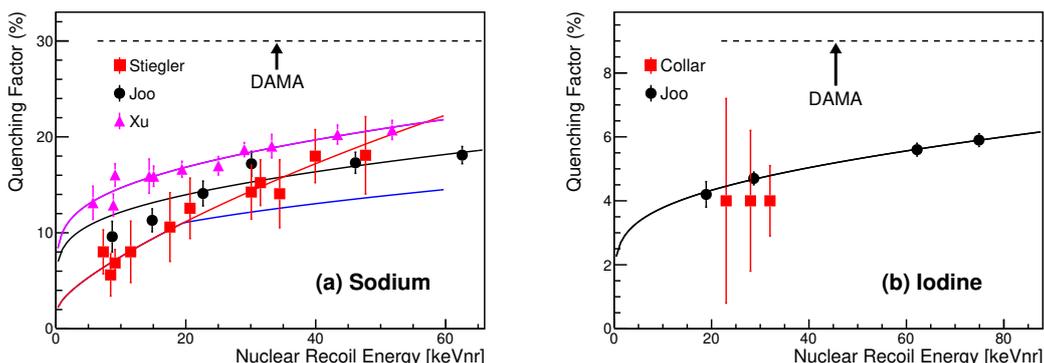
Figure 1. The nuclear recoil quenching factors of Na (a) and I (b) recoils in the NaI(Tl) crystal measured by DAMA [47] (black dashed line) are compared with the recent measurements by Stiegler *et al.* [50] (red square points), Xu *et al.* [49] (magenta triangle points) and Joo *et al.* [51] (black circle points). The new measurements are modeled with an empirical formula based on the Lindhard *et al.* model [57]. The blue solid line in (a) indicates our assumed lower bound of QF systematic uncertainty for $E_R \gtrsim 19.6$ keVnr that considers the fast increase of QF_{Na} in the Stiegler *et al.* data.

Measurement		p_0	p_1
Sodium	Xu *et al.*	$(7.18 \pm 1.22) \times 10^{-2}$	$(9.98 \pm 6.20) \times 10^{-3}$
	Joo *et al.*	$(5.88 \pm 0.75) \times 10^{-2}$	$(9.12 \pm 3.16) \times 10^{-3}$
	Stiegler *et al.*	$(9.25 \pm 5.97) \times 10^{-3}$	$(3.63 \pm 3.34) \times 10^{-1}$
Iodine	Joo *et al.*	$(1.94 \pm 0.44) \times 10^{-2}$	$(4.43 \pm 3.76) \times 10^{-3}$

Table 1. The fit results of the new QF measurements modeled by modified Lindhard *et al.* model [57] as shown in Fig. 1.
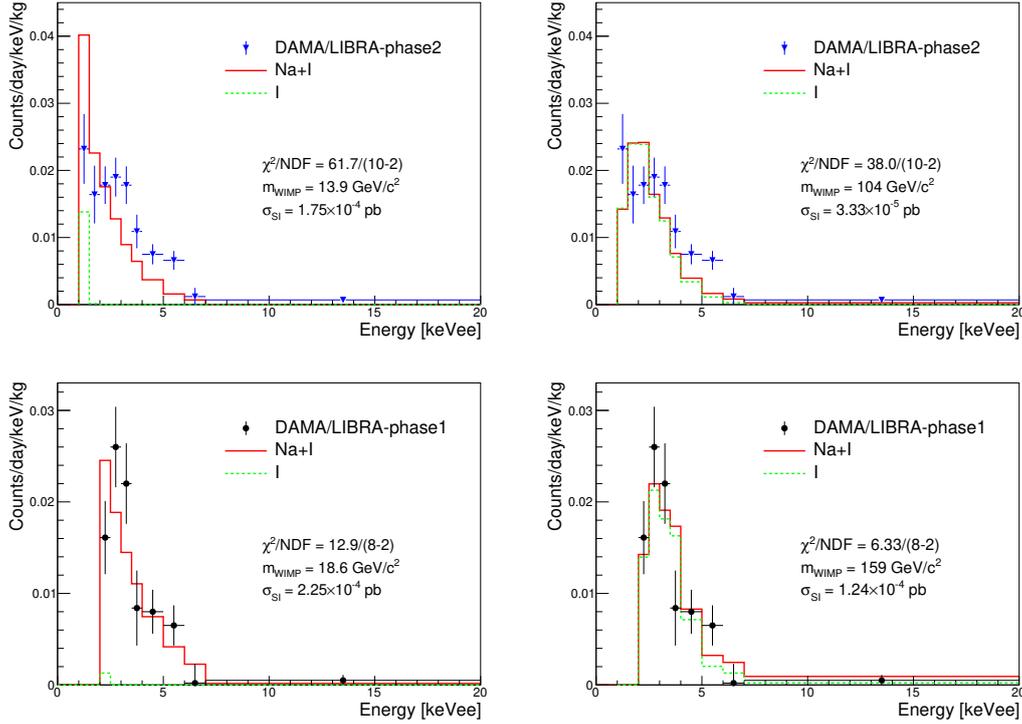
Figure 2. DAMA/LIBRA's modulation amplitudes (phase2:top and phase1:bottom) as a function of measured electron-equivalent energy are presented for low-mass regions (left) and high-mass regions (right) with the best fit models (red solid line), with the assumption of canonical SI WIMP interactions and the new QF values. The iodine-only component is denoted by the green-dashed line. The DAMA/LIBRA-phase1 data provide good fits for both low-mass and high-mass regions, while the phase2 data has large chi-squared values at the best fit points.

values from their maxima.

3 Isospin-conserving spin-independent interaction

For the DAMA/LIBRA-phase1 data, the isospin conserving SI scattering with DAMA QF values provided a good fit for WIMPs [35]. On the other hand, the observed DAMA/LIBRA-phase2 modulation data does not provide a good fit to the expectations for this model [39–41]. Switching to the new QF values for both the phase1 and phase2 data does not improve the phase2 data's agreement with the model, as shown in Fig. 2 and summarized in Table 2. As discussed in Ref. [39], modulation amplitude in the low-WIMP-mass allowed region, which

is dominated by WIMP-sodium scattering, is expected to increase rapidly for recoil energies below 1.5 keVee because of the onset of contributions from WIMP-iodine scattering. On the other hand, modulation amplitude in the the high-WIMP-mass allowed region, which is dominated by WIMP-iodine scattering, is expected to decrease at energies below 1.5 keVee. Since the DAMA/LIBRA-phase2 data displays a modulation amplitude that smoothly increases with energy below 1.5 keVee, the canonical SI WIMP interaction cannot provide a good fit to the phase2 data. We, therefore, only use the phase1 data for the interpretation of the canonical SI WIMP scattering with the new QF values. As shown in Fig. 3, the best fit regions of the DAMA/LIBRA-phase1 data with the new QF results show significantly increased values for both the allowed WIMP masses and WIMP-nucleon cross-sections. We find that the local minimum value of chi-squared with the new QF values in the low-mass region increases somewhat, while the chi-squared value for the high-mass region decreases, as summarized in Table 2.

The 90% confidence level (CL) upper limits for the COSINE-100 data are determined using the Bayesian method described in Ref. [34]. Even though the allowed parameter space from the DAMA/LIBRA-phase1 data is changed by the new QF values, the COSINE-100 results still exclude the DAMA 3σ region as shown in Fig. 3. This is because the dependence on QF values is nearly the same for the DAMA/LIBRA and COSINE-100 measurements.
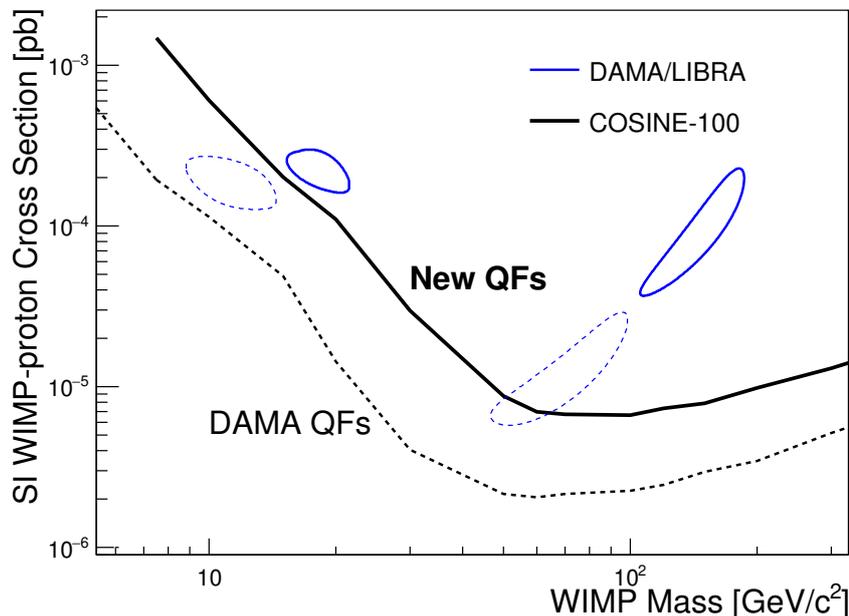
Figure 3. The 3σ allowed regions of the WIMP mass and the WIMP-proton cross-section associated with the DAMA/LIBRA-phase1 data (blue solid contours) are compared with the 90% CL upper limit from the COSINE-100 data (black solid line) with the new QF values. To illustrate the effects of the QF changes, we present the 3σ regions of the DAMA/LIBRA-phase1 data (blue dashed contours) and 90% CL limit of the COSINE-100 data (black dashed line) using the DAMA QF values (from Ref. [34]).
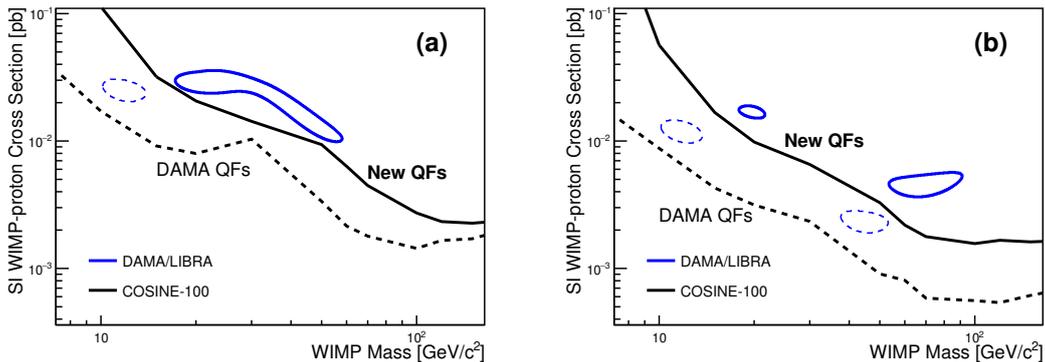
Figure 4. The 3σ allowed regions of the WIMP mass and the cross-section associated with the DAMA/LIBRA-phase1+phase2 data (blue solid contour) are compared with the 90% CL upper limit from the COSINE-100 data (black solid line). The dashed curves shown the results using the DAMA QF values. In each plot, we fix the effective coupling ratios to neutrons and protons f_n/f_p to their best fit values: (a) $f_n/f_p = -0.758$ (-0.756) for the low-mass regions and new (DAMA) QF values; (b) $f_n/f_p = -0.712$ (-0.684) for the high-mass regions and new (DAMA) QF values.

4 Isospin violating spin-independent interaction

It is clear from the above disussion that in order to fit both the DAMA/LIBRA-phase1 and phase2 data (DAMA/LIBRA-phase1+phase2 data), the contributions from WIMP-iodine scattering have to be suppressed. This can be accomplished if the WIMP-proton coupling is different from the WIMP-neutron coupling (isospin violating interaction) [39, 40]. (Sodium has nearly equal numbers of protons (11) and neutrons (12); iodine has 74 neutrons and 53 protons.) In this case, three parameters are used to fit the DAMA/LIBRA data: the WIMP mass, the WIMP-proton scattering cross-section, and the ratio between the effective coupling of WIMPs to neutrons and to protons (f_n/f_p). Figure 4 shows the 3σ-allowed WIMP mass vs. cross-sections regions for the DAMA/LIBRA-phase1+phase2 data with the new QF values for the best fit values of $f_n/f_p = -0.758$ (a) in the low-mass and $f_n/f_p = -0.712$ (b) in the high-mass regions. The low-mass and high-mass local minima are significantly shifted with respect to the results using the DAMA QF values. The minimum chi-squared values with the new QF values, listed in Table 2, indicate that this model provides a good description of the full DAMA/LIBRA-phase1+phase2 data set.

The 90% CL upper limits evaluated from the COSINE-100 data with f_n/f_p values determined from the best fit to the DAMA/LIBRA-phase1+phase2 data, shown in Fig. 4, exclude the allowed 3σ regions from the DAMA/LIBRA data. In a scan of different f_n/f_p values over the [-1,1] interval, we find the limits obtained from the COSINE-100 exclude the DAMA/LIBRA allowed 3σ regions for all cases.

5 Spin-dependent interaction

We use the effective field theory treatment and nuclear form factors from Ref. [62–64] to estimate the DAMA/LIBRA allowed regions for spin-dependent (SD) interactions using the publicly available DMDD package [65, 66]. In the fit to the DAMA/LIBRA data, we vary two parameters: the WIMP-mass and the WIMP-nucleon SD interaction cross section for

four cases in terms of ratio between WIMP-neutron and WIMP-proton SD couplings a_n/a_p (WIMP-proton/neutron only and $a_n/a_p = \pm 1$).

In case of the WIMP-neutron only SD interaction ($a_p=0$), the observed DAMA/LIBRA modulation data does not provide a good fit as shown in Table 2. In Fig. 5 (b) it is drawn for the completeness based on likelihood ratio. On the other hand, two local minima are obtained with the new QF values for the SD WIMP-proton interaction and other two mixed couplings, while only a low-mass WIMP has a good fit for the DAMA QF values as shown in Fig. 5. However, the chi-squared value of the best fit using the new QF values is slightly worse, as shown in Table 2. In the high-mass region, the relatively large chi-squared value with the new QF values corresponds to a similar trend seen in the fit that uses the DAMA QF values.

Figure 5 shows the 90% CL upper limits obtained from the COSINE-100 data with the same effective field theory treatment and nuclear form factors for sodium and iodine. The DAMA/LIBRA 3σ allowed regions for SD WIMP-proton interaction hypothesis are excluded by the 90% CL upper limit from the COSINE-100 data.
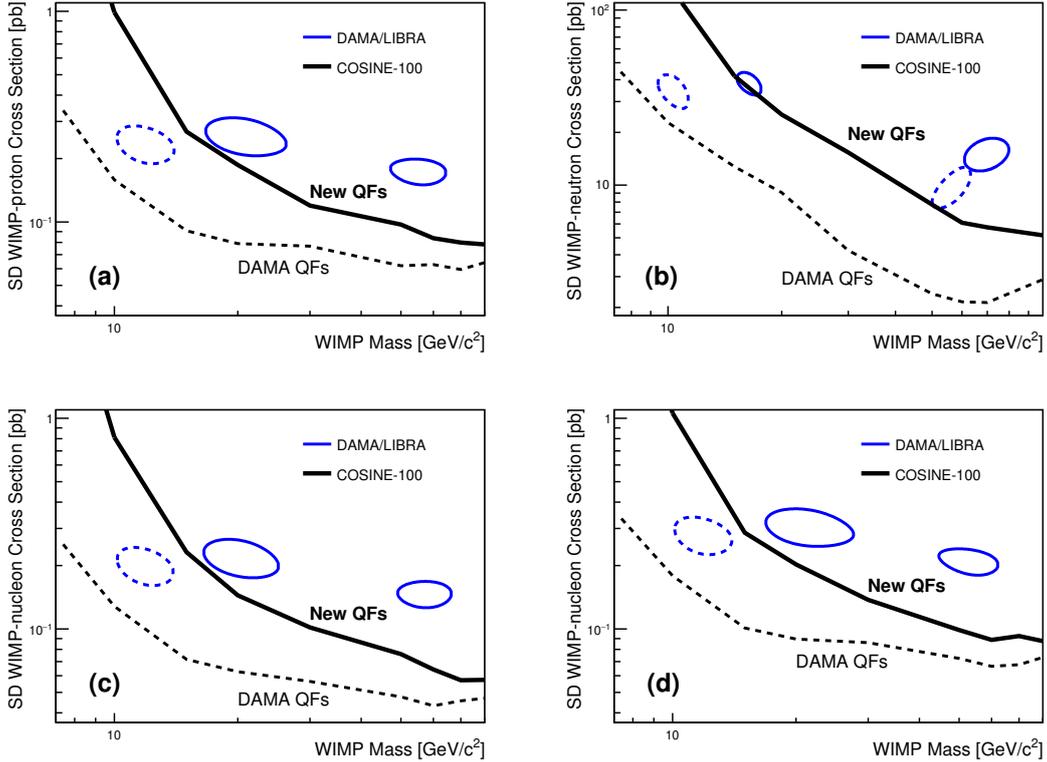
Figure 5. The 3σ allowed regions of WIMP mass vs. WIMP-nucleon SD cross-section associated with the DAMA/LIBRA-phase1+phase2 data (blue solid coutours) are compared with the 90% CL upper limit from the COSINE-100 data (black solid lines). These results use the new QF values; the dashed curves show the results using the DAMA QF values. (a) proton only (b) neutron only (c) $a_n/a_p = +1$ (d) $a_n/a_p = -1$.

6 Discussion

We examine the compatibility of the DAMA/LIBRA and COSINE 100 data in the context of various WIMP dark matter interaction hypotheses and taking into account the recently measured nuclear recoil QF values for sodium and iodine. Here we assume the standard galatic WIMP halo model with astrophysical parameters: $\rho_\chi = 0.3$ GeV/cm^3, $v_E = 232$ km/s, $\sqrt{2}\sigma_v = 220$ km/s, and $v_{esc} = 544$ km/s. We find that the DAMA/LIBRA-phase2 data are not compatible with canonical SI WIMP interaction in the context of the standard WIMP galactic halo model using the new QF values. Moreover, the DAMA/LIBRA-phase1 data only are well fitted but with significant shifts in both the allowed WIMP-mass and WIMP-nucleon cross-section values. We successfully obtained allowed regions from the DAMA/LIBRA-phase1+phase2 data for an isospin-violating interaction hypothesis, as well as for spin-dependent WIMP-proton and mixed couplings of proton and neutron interactions with the new QF values. However, for all the WIMP-dark matter interpretations of the DAMA/LIBRA data considered here, the COSINE-100 limits based on the initial 59.5 days' exposure exclude the 3σ allowed regions for the DAMA/LIBRA modulation signal at the 90% CL. Because the COSINE-100 experiment uses the same NaI(Tl) target medium as the DAMA/LIBRA experiment, this result strongly constrains models that purport to explain the DAMA/LIBRA modulation signal as being due to interactions of WIMPs in the galactic dark matter halo with nuclides in NaI(Tl) crystal detectors.

Acknowledgments

References

[1] D. Clowe et al., *A direct empirical proof of the existence of dark matter*, *Astrophys. J.* **648** (2006) L109.

[2] PLANCK collaboration, *Planck 2018 results. VI. Cosmological parameters*, 1807.06209.

[3] B. W. Lee and S. Weinberg, *Cosmological lower bound on heavy-neutrino masses*, *Phys. Rev. Lett.* **39** (1977) 165.

[4] G. Jungman, M. Kamionkowski and K. Griest, *Supersymmetric dark matter*, *Phys. Rept.* **267** (1996) 195.

[5] M. W. Goodman and E. Witten, *Detectability of Certain Dark Matter Candidates*, *Phys. Rev. D* **31** (1985) 3059.

[6] PARTICLE DATA GROUP collaboration, *Review of Particle Physics*, *Phys. Rev.* **D98** (2018) 030001.

[7] DAMA collaboration, *Searching for WIMPs by the annual modulation signature*, *Phys. Lett. B* **424** (1998) 195.

[8] DAMA collaboration, *First results from DAMA/LIBRA and the combined results with DAMA/NaI*, *Eur. Phys. J. C* **56** (2008) 333 [0804.2741].

[9] DAMA/LIBRA collaboration, *New results from DAMA/LIBRA*, *Eur. Phys. J. C* **67** (2010) 39 [1002.1028].

[10] DAMA/LIBRA collaboration, *Final model independent result of DAMA/LIBRA-phase1*, *Eur. Phys. J. C* **73** (2013) 2648 [1308.5109].

[11] DAMA/LIBRA collaboration, *First Model Independent Results from DAMA/LIBRA-Phase2*, *Nucl. Phys. At. Energy* **19** (2018) 307 [1805.10486].

[12] J. Lewin and P. Smith, *Review of mathematics, numerical factors, and corrections for dark matter experiments based on elastic nuclear recoil*, *Astropart. Phys.* **6** (1996) 87.

[13] K. Freese, J. A. Frieman and A. Gould, *Signal Modulation in Cold Dark Matter Detection*, *Phys. Rev. D* **37** (1988) 3388.

[14] S. C. Kim et al., *New Limits on Interactions between Weakly Interacting Massive Particles and Nucleons Obtained with CsI(Tl) Crystal Detectors*, *Phys. Rev. Lett.* **108** (2012) 181301 [1204.2646].

[15] CRESST-II collaboration, *Results on low mass WIMPs using an upgraded CRESST-II detector*, *Eur. Phys. J.* **C74** (2014) 3184 [1407.3146].

[16] SuperCDMS collaboration, *Search for Low-Mass Weakly Interacting Massive Particles with SuperCDMS*, *Phys. Rev. Lett.* **112** (2014) 241302 [1402.7137].

[17] XMASS collaboration, *Direct dark matter search by annual modulation in XMASS-I*, *Phys. Lett. B* **759** (2016) 272 [1511.04807].

[18] LUX collaboration, *Results from a Search for Dark Matter in the Complete LUX Exposure*, *Phys. Rev. Lett.* **118** (2017) 021303.

[19] XENON collaboration, *Search for Electronic Recoil Event Rate Modulation with 4 Years of XENON100 Data*, *Phys. Rev. Lett.* **118** (2017) 101101 [1701.00769].

[20] SuperCDMS collaboration, *Results from the Super Cryogenic Dark Matter Search Experiment at Soudan*, *Phys. Rev. Lett.* **120** (2018) 061802 [1708.08869].

[21] XENON collaboration, *Dark Matter Search Results from a One Tonne×Year Exposure of XENON1T*, *Phys. Rev. Lett.* **121** (2018) 111302 [1805.12562].

[22] DarkSide collaboration, *Low-Mass Dark Matter Search with the DarkSide-50 Experiment*, *Phys. Rev. Lett.* **121** (2018) 081307 [1802.06994].

[23] LUX collaboration, *Search for annual and diurnal rate modulations in the LUX experiment*, *Phys. Rev. D* **98** (2018) 062005 [1807.07113].

[24] CRESST collaboration, *First results from the CRESST-III low-mass dark matter program*, 1904.00498.

[25] K. W. Kim et al., *Tests on NaI(Tl) crystals for WIMP search at the Yangyang Underground Laboratory*, *Astropart. Phys.* **62** (2015) 249 [`1407.1586`].

[26] SABRE collaboration, *The SABRE project and the SABRE Proof-of-Principle*, *Eur. Phys. J. C* **79** (2019) 363 [`1806.09340`].

[27] COSINE-100 collaboration, *Initial Performance of the COSINE-100 Experiment*, *Eur. Phys. J. C* **78** (2018) 107 [`1710.05299`].

[28] K.-I. Fushimi, *Low Background Measurement by Means of NaI(Tl) Scintillator: Improvement of Sensitivity for Cosmic Dark Matter*, *RADIOISOTOPES* **67** (2018) 101.

[29] I. Coarasa et al., *ANAIS-112 sensitivity in the search for dark matter annual modulation*, *Eur. Phys. J. C* **79** (2019) 233 [`1812.02000`].

[30] J. Amare et al., *Performance of ANAIS-112 experiment after the first year of data taking*, *Eur. Phys. J. C* **79** (2019) 228 [`1812.01472`].

[31] COSINE-100 collaboration, *Background model for the NaI(Tl) crystals in COSINE-100*, *Eur. Phys. J. C* **78** (2018) 490.

[32] KIMS collaboration, *Performance of a prototype active veto system using liquid scintillator for a dark matter search experiment*, *Nucl. Instrum. Meth. A* **851** (2017) 103.

[33] COSINE-100 collaboration, *Muon detector for the COSINE-100 experiment*, *JINST* **13** (2018) T02007.

[34] COSINE-100 collaboration, *An experiment to search for dark-matter interactions using sodium iodide detectors*, *Nature* **564** (2018) 83 [`1906.01791`].

[35] C. Savage, G. Gelmini, P. Gondolo and K. Freese, *Compatibility of DAMA/LIBRA dark matter detection with other searches*, *JCAP* **0904** (2009) 010 [`0808.3607`].

[36] COSINE-100 AND SOGANG PHENOMENOLOGY GROUP collaboration, *COSINE-100 and DAMA/LIBRA-phase2 in WIMP effective models*, *JCAP* **1906** (2019) 048 [`1904.00128`].

[37] J. Amare et al., *First results on dark matter annual modulation from ANAIS-112 experiment*, *Phys. Rev. Lett.* **123** (2019) 031301 [`1903.03973`].

[38] COSINE-100 collaboration, *Search for a dark matter-induced annual modulation signal in NaI(Tl) with the COSINE-100 experiment*, *Phys. Rev. Lett.* **123** (2019) 031302 [`1903.10098`].

[39] S. Baum, K. Freese and C. Kelso, *Dark Matter implications of DAMA/LIBRA-phase2 results*, *Phys. Lett. B* **789** (2019) 262 [`1804.01231`].

[40] S. Kang, S. Scopel, G. Tomar and J.-H. Yoon, *DAMA/LIBRA-phase2 in WIMP effective models*, *JCAP* **1807** (2018) 016 [`1804.07528`].

[41] J. Herrero-Garcia, A. Scaffidi, M. White and A. G. Williams, *Time-dependent rate of multicomponent dark matter: Reproducing the DAMA/LIBRA phase-2 results*, *Phys. Rev. D* **98** (2018) 123007 [`1804.08437`].

[42] A. A. Klypin, S. Trujillo-Gomez and J. Primack, *Dark Matter Halos in the Standard Cosmological Model : Results from the Bolshoi Simulation*, *Astrophys. J.* **740** (2011) 102.

[43] A. M. Green, *Astrophysical uncertainties on the local dark matter distribution and direct detection experiments*, *J. Phys.* **G44** (2017) 084001 [1703.10102].

[44] Y. Wu, K. Freese, C. Kelso, P. Stengel and M. Valluri, *Uncertainties in Direct Dark Matter Detection in Light of Gaia*, 1904.04781.

[45] R. Bernabei et al., *Improved model-dependent corollary analyses after the first six annual cycles of DAMA/LIBRA-phase2*, 1907.06405.

[46] M. R. Buckley, G. Mohlabeng and C. W. Murphy, *Direct Detection Anomalies in light of Gaia Data*, *Phys. Rev.* **D100** (2019) 055039 [1905.05189].

[47] DAMA collaboration, *New limits on WIMP search with large-mass low-radioactivity NaI(Tl) set-up at Gran Sasso*, *Phys. Lett. B* **389** (1996) 757 .

[48] J. I. Collar, *Quenching and channeling of nuclear recoils in NaI(Tl): Implications for dark-matter searches*, *Phys. Rev. C* **88** (2013) 035806 [1302.0796].

[49] J. Xu et al., *Scintillation Efficiency Measurement of Na Recoils in NaI(Tl) Below the DAMA/LIBRA Energy Threshold*, *Phys. Rev. C* **92** (2015) 015807 [1503.07212].

[50] T. Stiegler, C. Sofka, R. C. Webb and J. T. White, *A study of the NaI(Tl) detector response to low energy nuclear recoils and a measurement of the quenching factor in NaI(Tl)*, 1706.07494.

[51] H. W. Joo, H. S. Park, J. H. Kim, S. K. Kim, Y. D. Kim, H. S. Lee et al., *Quenching factor measurement for NaI(Tl) scintillation crystal*, *Astropart. Phys.* **108** (2019) [1809.10310].

[52] N. J. C. Spooner, G. J. Davies, J. D. Davies, G. J. Pyle, T. D. Bucknell, G. T. A. Squier et al., *The Scintillation efficiency of sodium and iodine recoils in a NaI(Tl) detector for dark matter searches*, *Phys. Lett. B* **321** (1994) 156.

[53] G. Gerbier, J. Mallet, L. Mosca, C. Tao, B. Chambon, V. Chazal et al., *Pulse shape discrimination with NaI(Tl) and results from a WIMP search at the Laboratoire Souterrain de Modane*, *Astropart. Phys.* **11** (1999) 287.

[54] T. Jagemann, F. Feilitzsch and J. Jochum, *Measurement of the scintillation light quenching at room temperature of sodium recoils in NaI(Tl) and hydrogen recoils in NE 213 by the scattering of neutrons*, *Nucl. Instrum. Meth. A* **564** (2006) 549.

[55] E. Simon et al., *SICANE: A Detector array for the measurement of nuclear recoil quenching factors using a monoenergetic neutron beam*, *Nucl. Instrum. Meth. A* **507** (2003) 643 [astro-ph/0212491].

[56] H. Chagani, P. Majewski, E. J. Daw, V. A. Kudryavtsev and N. J. C. Spooner, *Measurement of the quenching factor of Na recoils in NaI(Tl)*, *JINST* **3** (2008) P06003 [0806.1916].

[57] J. Lindhard, V. Nielsen, M. Scharff and P. Thomsen, *Integral equations governing radiation effects. (Notes on Atomic collisions, III)*, Mat. Fys. Medd. Dan. Vid. Selsk. **33** (1963) .

[58] K. Ianakiev, B. Alexandrov, P. Littlewood and M. Browne, *Temperature behavior of NaI(Tl) scintillation detectors*, *Nucl. Instrum. Meth. A* **607** (2009) 432 [`physics/0605248`].

[59] COSINE-100 collaboration, *The COSINE-100 Data Acquisition System*, *JINST* **13** (2018) P09006 [`1806.09788`].

[60] DAMA/LIBRA collaboration, *The DAMA/LIBRA apparatus*, *Nucl. Instrum. Meth. A* **592** (2008) 297.

[61] DAMA/LIBRA collaboration, *Performances of the new high quantum efficiency PMTs in DAMA/LIBRA*, *JINST* **7** (2012) P03009.

[62] A. L. Fitzpatrick, W. Haxton, E. Katz, N. Lubbers and Y. Xu, *The Effective Field Theory of Dark Matter Direct Detection*, *JCAP* **1302** (2013) 004 [`1203.3542`].

[63] N. Anand, A. L. Fitzpatrick and W. C. Haxton, *Weakly interacting massive particle-nucleus elastic scattering response*, *Phys. Rev. C* **89** (2014) 065501 [`1308.6288`].

[64] M. I. Gresham and K. M. Zurek, *Effect of nuclear response functions in dark matter direct detection*, *Phys. Rev. D* **89** (2014) 123521 [`1401.3739`].

[65] V. Gluscevic and S. D. McDermott, "dmdd: Dark matter direct detection." Astrophysics Source Code Library [ascl:1506.002], 2015.

[66] V. Gluscevic, M. I. Gresham, S. D. McDermott, A. H. G. Peter and K. M. Zurek, *Identifying the Theory of Dark Matter with Direct Detection*, *JCAP* **1512** (2015) 057 [`1506.04454`].

Model	QF	χ^2/NDF	m_{WIMP} [GeV/c^2]	σ_{WIMP} [pb]	f_n/f_p
Canonical SI (Phase1 only)	**New**	12.9/(8-2) (2.0σ)	18.6	2.25×10^{-4}	
		6.33/(8-2) (0.9σ)	159	1.24×10^{-4}	
	DAMA	9.62/(8-2) (1.5σ)	11.3	1.96×10^{-4}	1.000
		7.51/(8-2) (1.1σ)	75.5	1.40×10^{-5}	
Canonical SI (Phase2 only)	**New**	61.7/(10-2) (6.0σ)	13.9	1.75×10^{-4}	
		38.0/(10-2) (4.5σ)	104	3.33×10^{-5}	
	DAMA	51.6/(10-2) (5.6σ)	8.96	1.61×10^{-4}	1.000
		20.2/(10-2) (2.6σ)	59.6	8.41×10^{-6}	
Isospin violating SI (Phase1+2)	**New**	19.4/(18-3) (1.3σ)	19.5	2.90×10^{-2}	-0.758
		17.5/(18-3) (1.1σ)	69.2	4.55×10^{-3}	-0.712
	DAMA	17.1/(18-3) (1.0σ)	11.8	2.54×10^{-2}	-0.756
		17.4/(18-3) (1.0σ)	44.6	2.36×10^{-3}	-0.684
WIMP-proton SD (Phase1+2)	**New**	24.2/(18-2) (1.7σ)	20.7	2.59×10^{-1}	
		30.5/(18-2) (2.4σ)	55.6	1.74×10^{-1}	
	DAMA	17.3/(18-2) (0.9σ)	11.8	2.37×10^{-1}	-
		45.2/(18-2) (3.8σ)	42.3	1.55×10^{-1}	
WIMP-neutron SD (Phase1+2)	**New**	50.8/(18-2) (4.3σ)	16.4	3.83×10	
		44.0/(18-2) (3.7σ)	69.6	1.52×10	
	DAMA	37.5/(18-2) (3.1σ)	10.4	3.50×10	-
		36.6/(18-2) (3.0σ)	56.7	9.89	
mixed SD: $a_n = a_p$ (Phase1+2)	**New**	25.8/(18-2) (1.9σ)	20.2	2.20×10^{-1}	
		31.7/(18-2) (2.5σ)	57.4	1.47×10^{-1}	
	DAMA	17.2/(18-2) (0.9σ)	11.8	2.02×10^{-1}	-
		41.2/(18-2) (3.5σ)	44.1	1.24×10^{-1}	
mixed SD: $a_n = -a_p$ (Phase1+2)	**New**	22.8/(18-2) (1.6σ)	21.2	3.09×10^{-1}	
		29.2/(18-2) (2.3σ)	53.4	2.10×10^{-1}	
	DAMA	17.6/(18-2) (0.9σ)	11.8	2.81×10^{-1}	-
		52.2/(18-2) (3.4σ)	40.4	1.98×10^{-1}	

Table 2.   The best fit values for the comparison of six WIMP-nucleon interaction hypotheses to the DAMA/LIBRA data are summarized. Here we present the fit results based on both the DAMA and new QF values. The first and second groups of rows are for the canonical SI interaction using the phase1 and phase2 data, respectively. The other groups use the DAMA/LIBRA-phase1+phase2 data for the fit. The third group is for the isospin-violating SI interaction while the next four groups are for the SD interactions. The SD interactions are shown for proton only interaction (fifth group), neutron only interaction (sixth group), and mixed couplings of a_n/a_p=1 (seventh group) and $a_n/a_p =$ -1 (eight group). The canonical SI interaction for the DAMA/LIBRA-phase2 data and neutron only SD interaction do not provide good fits, while for the other cases good fits are obtained.